An adaptive network model for a possible therapy for the effects of a certain type of dementia on social functioning

Commu, Charlotte; Treur, Jan; Dols, Annemieke; Pijnenburg, Yolande A.L.

published in
Biologically Inspired Cognitive Architectures
2018

DOI (link to publisher)
10.1016/j.bica.2018.10.002

document version
Publisher's PDF, also known as Version of record

Biologically Inspired Cognitive Architectures 26 (2018) 145–158

Contents lists available at ScienceDirect

Biologically Inspired Cognitive Architectures

journal homepage: www.elsevier.com/locate/bica

Research article

An adaptive network model for a possible therapy for the effects of a certain type of dementia on social functioning

Charlotte Commu[a], Jan Treur[a,*], Annemieke Dols[b,c], Yolande A.L. Pijnenburg[b]

[a] Behavioural Informatics Group, Department of Computer Science, Vrije Universiteit Amsterdam, The Netherlands
[b] Ouderenpsychiatrie, GGZ inGeest, Amsterdam, The Netherlands
[c] Alzheimer Centre, VUmc, Amsterdam, The Netherlands

ARTICLE INFO

Keywords:
Adaptive network model
Dementia
Social functioning

ABSTRACT

This paper first describes a temporal-causal network model for recognition of emotions shown by others. The model can show both normal functioning and dysfunctioning, such as can be the case with certain types of dementia. More specifically the focus of the paper is on a specific type of therapy that has been incorporated in the model (thus becoming adaptive) to study the effects and potentials of this therapy to improve the dysfunctional behaviour. Simulations have been performed to test the model. A mathematical analysis was done which gave evidence that the model as implemented does what it is meant to do. The model can be applied to obtain a virtual patient model to study the way in which recognition of emotions can deviate for certain types of persons, and what a therapy can contribute to improve the situation.

Introduction

Computational methods are used more and more often to get insight into human functioning and dysfunctioning. By designing a human-like computational model for normal functioning of certain mental and/or social processes, it can be explored what alterations make the model show dysfunctional behavior, and verify how that relates to the empirical literature. Such a computational model can be a basis for a so-called virtual patient model. An important source of knowledge for the design of a human-like computational model is found in the fields of Cognitive and Social Neuroscience, and in what is encountered in the practice of medical clinics. The work reported in this paper results from a cooperation between researchers in AI and in medical practice.

The focus of this study is on social functioning and dysfunctioning resulting from a certain type of dementia, in particular the behavioral variant of frontotemporal dementia (bvFTD); see (Piguet, Hornberger, Mioshi, & Hodges, 2011), and on the effect of a certain type of therapy. As will be explained in Section 2 in more detail, one of the problems encountered is difficulty in recognizing emotions of others, in particular the negative ones, even while emotion contagion can still function properly.

To model such human processes in a way that is justifiable from a neuroscientific perspective, knowledge of the underlying mechanisms in the brain is necessary. Dynamics and cyclic connections play an important role in such brain mechanisms, and therefore a modeling approach is needed that can handle cyclic dynamic processes. The Network-Oriented Modeling approach based on temporal-causal networks used here is able to satisfy these needs (Treur, 2016b; Treur, 2018).

In this paper, the first part focuses on creating the model, experimenting with the model and verifying the model. First, Section 2 contains background knowledge on the processes addressed and on the therapy that was addressed. In Section 3 the basic temporal-causal network model is introduced. Section 4 describes the simulation experiments for the addressed case, both for normal functioning and for dysfunctioning. Section 5 shows how the addition of a certain type of therapy (repetitive Transcranial Magnetic Stimulation: rTMS) leads to an adaptive network model. Section 6 describes the simulation experiments for the adaptive model with this therapy. Section 7 describes how the adaptive model was verified by mathematical analysis. Section 8 is a discussion. Finally, Section 9 concludes the paper.

Neuropsychiatric background of bvFTD and a therapy

In the Netherlands, over 270.000 people have dementia. After cancer and heart- and vascular diseases it is the most common cause of death. The majority of people that suffer from dementia (70%) have the most common form: Alzheimer's disease. No cures for the disease have been found yet, and due to the aging of society its future perspective does not seem bright. Expectations are that over 500.000 people will have some form of dementia in 2040, in 2055 this number is expected to be over 690.000 (Alzheimer Nederland, 2017).

* Corresponding author.
E-mail addresses: j.treur@vu.nl (J. Treur), A.Dols@ggzingeest.nl (A. Dols), YAL.Pijnenburg@vumc.nl (Y.A.L. Pijnenburg).

https://doi.org/10.1016/j.bica.2018.10.002
Received 22 September 2018; Received in revised form 13 October 2018; Accepted 16 October 2018

Alzheimer's disease might be the most common form of dementia, but is certainly not the only one. One other form of dementia that can be distinguished is Frontotemporal Dementia. Frontotemporal dementia (FTD) is the second most common cause of early-onset dementia and exists in two forms: the behavioral variant of frontotemporal dementia (bvFTD), which concerns progressive deterioration in social function and personality, and primary progressive aphasia (PPA), which deals with a decline in language skills (Piguet et al., 2011). This paper focusses on the behavioral variant of frontotemporal dementia (bvFTD). The behavioral variant of frontotemporal dementia is a neurodegenerative disorder associated with progressive degeneration of the frontal lobes, temporal lobes, or both (Piguet et al., 2011, Rascovsky et al., 2011). These deal with the social functioning of a human and can be seen as the social center of your brain. The control of your behaviour lies in those areas, when these areas are damaged it affects your behaviour and personality.

The initial symptoms for someone that has bvFTD are not clearly present and only small changes are shown at the early stages. Moreover, symptoms that are present at the early stages have often much in common with other mental problems like depression, stress, adjustment problems or lapses of judgment and self-control (Eslinger, Moore, Antani, Anderson, & Grossman, 2012), which makes it hard to correctly connect the symptoms with the correct disease. An important aspect to pinpoint the onset of the disease is interviewing a close family member to evoke the start of the symptoms. Alterations in social cognitions represent the earliest and core symptoms of bvFTD and this results in emotional disengagement and socially inappropriate responses or activities (Ibanez & Manes, 2012; Kumfor & Hodges, 2017). One of those symptoms that slightly slips into the lives of someone that has bvFTD and his spouses is apathy and withdrawal from social activities. Someone seems less goal-driven and has difficulties initiating conversations (Lanata & Miller, 2016). Moreover, there is a lack of interest and progressive social isolation (Piguet & Hodges, 2013).

Another symptom is loss of empathy. Patients with bvFTD have difficulties interpreting and/or processing the emotional states of self and others. This results in a lack of self-awareness, but also a lack of empathy and sympathy towards others. Spouses of patients often report difficulties in connecting with the patient on an emotional level since they show less sympathy, are not able to understand social cues, and lack interpersonal warmth (Lanata & Miller, 2016; Piguet & Hodges, 2013).

One of the last core symptoms concerns disinhibition. Patients could show inappropriate behaviour in public and towards strangers such as offensive jokes, cursing, telling stories, hugging, and kissing. Also, behavioral acts such as impulsivity, gambling, excessive buying, criminal behaviour, or changes in eating preferences are seen within patients (Piguet et al., 2011; Lanata & Miller, 2016; Piguet & Hodges, 2013). In this paper, the following case, experienced in the clinic, is used as an illustration.

The case is as follows:

Box 1

The case on which the model is based on

> **Case**:
>
> A 55 year old man who was recently diagnosed with bvFTD visited our outpatient clinic with his wife. While explaining the difficulties she met in the home situation, she started crying. The patient followed the conversation, and at this point he looked at her, his own eyes got watery, but he looked dazzled. Upon the question how he thought his wife was feeling, he answered that his wife was probably feeling happy. On the Ekman 60 faces test, he scored 43 out of 60 items correctly, which is below the cutoff of 46. His subscores were: Anger 8/10, Disgust 9/10, Anxiousness 8/10, Happiness 8/10, Sadness 5/10, Surprise 5/10.

The case explains that in patients with bvFTD there may be a dissociation between emotion contagion and facial emotion recognition. Specifically, the recognition of sadness shown by others is particularly difficult. Some studies of social cognition in bvFTD have already shown that facial emotion recognition is disturbed, with the exception of happiness. For example, damaged recognition of negative emotions such as anger and disgust have been described (Gossink et al., 2018). As adopted from the medical experts (Commu, Treur, Dols, & Pijnenburg, 2018):

> "Applying the animal model of empathy of Frans de Waal, emotional contagiousness is the most inner layer, present from early evolution in most vertebrate animals (de Waal, 2009). Following the hypothesis that empathy in humans, and more specific in bvFTD, will exhibit a 'Recapitulati in reverse', the outlayers of the Russian Doll, symbolic for more advanced evolutionary social cognitive abilities will be lost first and the inner layer of emotion contagion will be preserved and even more prominent in advanced dementia: 'Heightened emotional contagion in mild cognitive impairment and Alzheimer's disease is associated with temporal lobe degeneration', by (Sturm et al., 2013), as is illustrated in this case."

As explained above, one of the core symptoms of bvFTD are changes in social cognition which results in inappropriate social behaviour and change of personality. For relatives of the patient, this symptom strikes the most as the patient changes as a person and might not be recognized as himself anymore. As of today, no cure has been found for bvFTD (Boxer & Boeve, 2007), while a delay of decline could make a crucial difference for a patient and its relatives.

Repetitive Transcranial Magnetic Stimulation (rTMS) is a method which can improve network efficacy in several neuropsychiatric disorders (Eldaief, Press, & Pascual-Leone, 2013). It is a technique in which brain activity is changed by using a short magnetic pulse. A small coil of wire is placed on the scalp to pass electrical energy across the scalp and skull. For example, when the coil is placed on the brain area that is responsible for movement of the thumb, the magnetic pulse causes the thumb to move. By using it repetitively, in this way, brain activity can be changed in the long term (Wassermann, 1998).

Repetitive TMS has been used successfully for many different subjects with psychiatric disorders such as depression, auditory verbal hallucinations, schizophrenia, and obsessive-compulsive disorder (Slotema, Dirk Blom, Hoek, & Sommer, 2010). Unfortunately, research in the field of dementia is limited. However, research that has been done has shown positive outcomes: improvements were found in alleviating neuropsychiatric symptoms and cognitive deficits (Elder & Taylor, 2014). Consequently, research in the field of rTMS with bvFTD is even more limited. As of today, one study has been performed in which rTMS therapy has been used on patients with diagnosed bvFTD. Results showed that rTMS may improve the cognitive performance and suggest that rTMS may also improve daytime functioning, but no improvements of mood were found (Antczak et al., 2018). However, this does not directly imply that social cognition improves as well.

The researchers in medical practice with whom a collaboration has been formed within this project have set up a research program to use rTMS to improve social functioning in bvFTD. In this part, it is hypothesised that for bvFTD patients rTMS will improve network efficacy of the social brain: when used for stimulation of the relevant areas it will strengthen the connections that were weakened by bvFTD. By designing a computational model including the rTMS therapy and its impacts, the effects of this therapy can be analysed computationally by simulation and evaluated for future purposes.

The temporal-causal network model

This section describes the temporal-causal network model for the interpretation of emotions. The model describes how interpretation of

emotions takes place, focussing on recognizing emotions shown by others. Patients with the behavioural variant of frontotemporal dementia (bvFTD) show emotional disengagement and social responses or activities that are not suitable. In particular, this model focuses on the part where people with bvFTD are unable to recognize and attribute emotional states to self and others. This can lead to the effect that emotions are misinterpreted or even not recognized. The model can both show how the process of recognizing and attributing emotional states works regularly and when it is affected by bvFTD.

A conceptual representation of a temporal-causal network model represents in a declarative manner states and connections between them that indicate (causal) impacts of states on each other, as assumed to hold for the application domain addressed. The states have (activation) levels that vary over time. The following three notions are main elements of a conceptual representation of a temporal-causal network model:

Connection weight $\omega_{X,Y}$ Each connection from a state X to a state Y has a *connection weight value* $\omega_{X,Y}$ representing the strength of the connection, between -1 and 1.
Combination function $\mathbf{c}_Y(..)$ For each state a *combination function* $\mathbf{c}_Y(..)$ to aggregate the causal impacts of other states on state Y.
Speed factor η_Y For each state Y a *speed factor* η_Y to represent how fast a state is changing upon causal impact.

The conceptual and numerical representation of the model introduced will be presented in this section. The model is designed by integrating a number of theories some of which were discussed in Section 2, and elements from Damasio (1994; 1999; 2018)'s view on emotions and feelings, and Iacoboni (2009) on mirror neurons and social contagion.

The developed model shows the difficulties that persons with bvFTD can have regarding recognition of emotions. Not only the recognition of emotions of others is included, but also the experience of own emotional feelings which includes mirror links from observed emotions. Fig. 1 gives an overview of the conceptual representation of the model. The following notations are used for the state names:

ws	world state
ss	sensor state
srs	sensory representation state
bs	belief state
ps	preparation state
cs	control state
es	execution state

For each state a label LP_n refers to the corresponding numerical representation of the update equation of the state, as described below. An overview of the states, their connections and weights can be found in Table 1. States or weights with subscript h or s correspond to the emotional feelings happy or sad. An example is ss_h meaning the sensor state for the own emotional response for happy (sensing the own body state, for example, the own smile). States indicated by a B correspond to the observation of emotional expression(s) of another person B. For example, $\mathrm{srs}_{B,h}$ means the sensory representation state of B having a happy face. Finally, subscript e is used to indicate if someone is showing any emotion. Therefore, $\mathrm{ws}_{B,e}$ means the world state of person B showing an emotion, for example, an emotional face. Overall, the upper part (the first three causal pathways) are used for recognizing the emotional state of someone else (person B).

The lower part (the other two causal pathways) is used to model feelings of own emotions using body loops and as-if body loops as described by Damasio (1994, 1999, 2018). The model presented here incorporates parts of the model described by (Treur, 2016b, Ch. 9). The part that is included from this model are the bottom two cycles of states with the body loops affecting the body state x of a person, representing own emotional feeling according to the theory of Damasio (1994, 1999, 2018). In this model, body state x can be either s (sad) or h (happy) corresponding to the emotion. This emotion can also be expressed by another person B. Therefore, the communication of, for example, body state h (happy) to B expresses that the person *self* knows that B feels h (happy). The connections from $\mathrm{srs}_{B,h}$ and $\mathrm{srs}_{B,s}$ to ps_h and ps_s, respectively, provide mirroring functionality to the preparation states, following Iacoboni's (2009) findings. These connections make the person feel what the other person expresses.

Most connection weights have a positive value between 0 and 1 according to the strength of the effect they have on consecutive states. However, suppressing effects are modeled by using a negative weight. A few of those negative weights occur in the model. The connection weights with a negative value are $\omega_{3,h,s}$, $\omega_{3,s,h}$, $\omega_{7,h,s}$, $\omega_{7,s,h}$, $\omega_{3,h}$, and $\omega_{3,s}$.

A conceptual representation of the temporal-causal network model can be transformed in a systematic manner into a numerical representation of the model (Treur, 2016b):

At each time point t each state X connected to state Y has an *impact* on Y defined as $\mathbf{impact}_{X,Y}(t) = \omega_{X,Y}X(t)$ where $\omega_{X,Y}$ is the weight of the connection from X to Y

Based on the combination function $\mathbf{c}_Y(...)$ the *aggregated impact* of multiple states X_i on Y at t is:

$$\begin{aligned}\mathbf{aggimpact}_Y(t) &= \mathbf{c}_Y(\mathbf{impact}_{X_1,Y}(t),\cdots,\mathbf{impact}_{X_k,Y}(t))\\ &= \mathbf{c}_Y\left(\omega_{X_1,Y}X_1(t),\cdots,\omega_{X_k,Y}X_k(t)\right)\end{aligned}$$

where X_i are the states with outgoing connections to state Y

Using the speed factor η_Y the effect of $\mathbf{aggimpact}_Y(t)$ on Y is exerted *over time gradually*:

$$Y(t+\Delta t) = Y(t) + \eta_Y[\mathbf{aggimpact}_Y(t) - Y(t)]\Delta t$$

or

$$\frac{dY(t)}{dt} = \eta_Y[\mathbf{aggimpact}_Y(t) - Y(t)]$$

Thus, the following *difference* and *differential equation* for Y are obtained:

$$Y(t+\Delta t) = Y(t) + \eta_Y\left[\mathbf{c}_Y\left(\omega_{X_1,Y}X_1(t),\cdots,\omega_{X_k,Y}X_k(t)\right) - Y(t)\right]\Delta t$$

$$\frac{dY(t)}{dt} = \eta_Y\left[\mathbf{c}_Y\left(\omega_{X_1,Y}X_1(t),\cdots,\omega_{X_k,Y}X_k(t)\right) - Y(t)\right]$$

The states related to LP1, LP2, LP3, LP6, LP7, LP11, LP12, LP16, LP19, LP20, LP23, LP24, and LP25 make use of the identity combination function $\mathbf{c}(V) = \mathbf{id}(V) = V$. Those for LP8, LP9, LP13, LP14, LP17, LP18, LP21, and LP22 make use of the scaled sum combination function, which is represented numerically by:

$$\mathbf{c}(V_1,\cdots,V_k) = \mathbf{ssum}_\lambda(V_1,\cdots,V_k) = \frac{V_1+\cdots+V_k}{\lambda}$$

where λ is the scaling factor. Finally, states related to LP10 and LP15 make use of a logistic function to get a binary all-or-nothing effect of these communications.

$$\mathbf{c}(V_1,\cdots,V_k) = \mathbf{alogistic}_{\sigma,\tau}(V_1,\cdots,V_k) = \left[\frac{1}{1+\mathbf{e}^{-\sigma(V_1+\cdots+V_k-\tau)}} - \frac{1}{1+\mathbf{e}^{\sigma\tau}}\right](1+\mathbf{e}^{-\sigma\tau})$$

Example simulation experiments for the model without therapy

To explore the behaviour of the designed temporal-causal network model, two scenarios were simulated in Matlab. The first scenario describes the case of how a person normally would recognize emotions shown by others. In this case, it is expected that when person B shows an emotion, the person will correctly communicate this emotion at the communication states $\mathrm{es}_{comm,B,h}$ or $\mathrm{es}_{comm,B,s}$. Also, the own feeling of

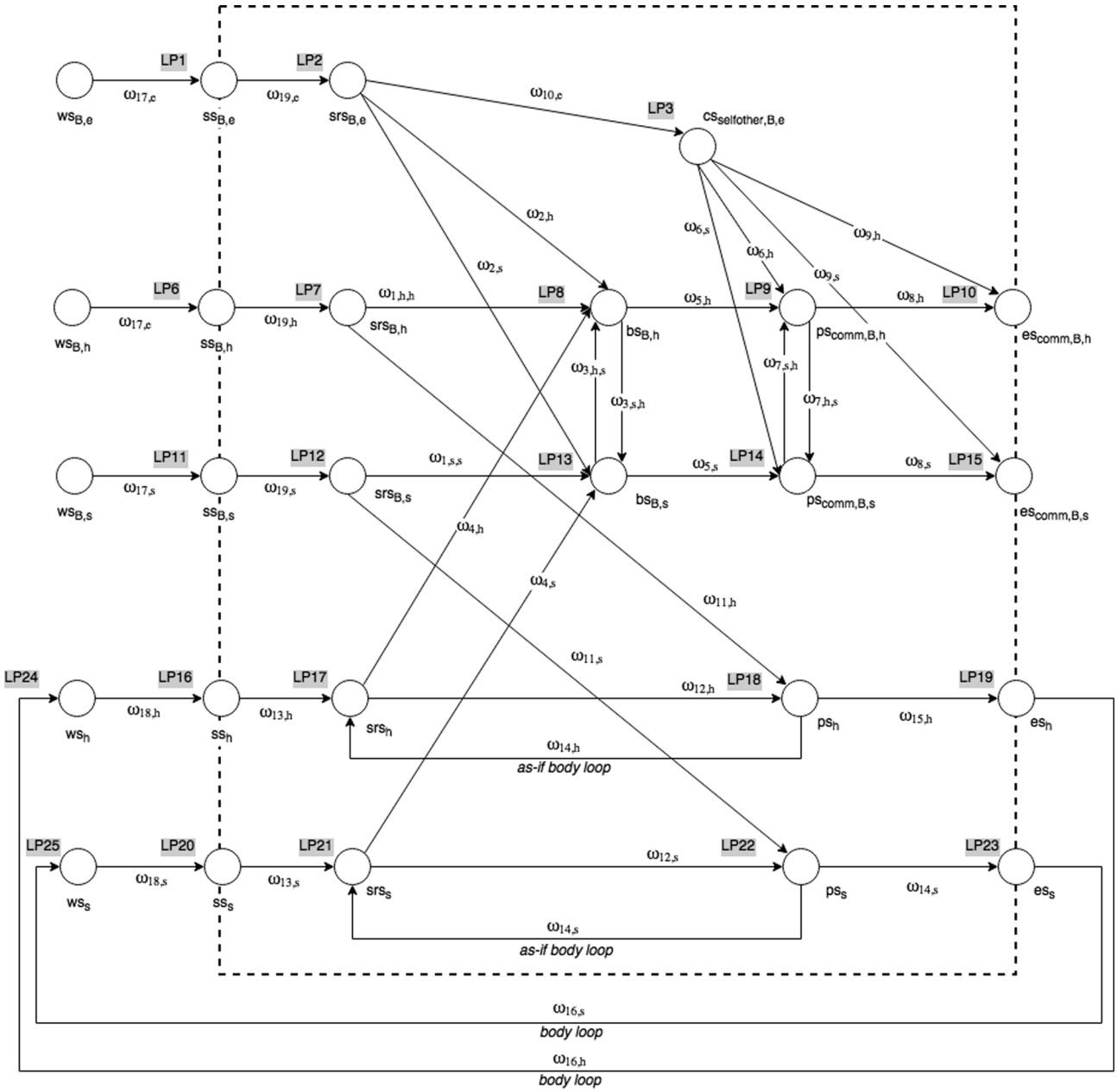

Fig. 1. Overview of the conceptual representation of the model.

that specific observed emotion will be activated through mirror neurons. The second scenario describes the specific case in which a person has difficulties recognizing the right emotions due to bvFTD. It is expected that when person *B* shows the emotion sad, this emotion will be wrongly interpreted by the patient with bvFTD as happy as explained by the case in Box 1. Therefore, the communication states will yield activations that differ from the ones in the first scenario, although through the mirroring system contagion still takes place through which the sadness is felt.

The weights for the connection strengths ω_k are for most connections set to 1; the exceptions are shown in the lower part of Table 2. For $\omega_{7,h,s}$ and $\omega_{7,s,h}$ a value of -0.2 has been chosen, since the preparation states for communication that either it is a sad emotion that person *B* is showing or a happy emotion normally will not have a high activation level at the same time. In this way, negative weights will cause suppression between the states if one of them is activated. Similarly, for weights $\omega_{3,h,s}$ and $\omega_{3,s,h}$ a value of -0.05 has been chosen, to express that the belief states for either believing person *B* shows a happy emotion or a sad emotion will usually not have high activations at the same time. Note that the values 0.7 and 0.05 for $\omega_{2,h}$ and $\omega_{2,s}$, respectively, indicate that when no specific emotion is recognized, usually an emotional face is more believed to indicate happiness than sadness.

The simulations have been performed with speed factor $\eta = 0.5$ for all states, $\Delta t = 0.5$, and the scaling factors as displayed in the upper part of Table 2. Since LP10 and LP15 make use of a logistic function, they have a threshold and steepness. Both states use a logistic function with steepness 200 and threshold 0.5. In the figures that show the results of the simulations, time can be seen on the horizontal axis of the figures and the activation levels of the states are on the vertical axis.

The graphs in Figs. 2–4 display the results of the simulations that have been performed for both scenarios. The graphs show a part of the results, to highlight the important states. A few of the states have the same color, as they are overlapping and follow the exact same development over time. Scenario 1 is divided into two different simulations. Difference between both simulations is the input and expected outcome. The first simulation describes a situation in which the input

Table 1
Overview of the connections, their weights, and their explanations; see also Fig. 1.

from state	to state	weight	connection	LP	explanation
$ws_{B,e}$	$ss_{B,e}$	$\omega_{17,e}$	sensing e of B	LP1	Sensing body state e (emotional) of person B
$ss_{B,e}$	$srs_{B,e}$	$\omega_{19,e}$	representing e of B	LP2	Representing the stimulus: B showing emotional
$srs_{B,e}$	$cs_{selfother,B,e}$	$\omega_{10,e}$	monitoring e of B	LP3	Control state for self-other distinction from represented emotion of person B
$ws_{B,h}$	$ss_{B,h}$	$\omega_{17,h}$	sensing h of B	LP6	Sensing body state h (happy) of person B
$ss_{B,h}$	$srs_{B,h}$	$\omega_{19,h}$	representing h of B	LP7	Representing the stimulus of B showing happy
$srs_{B,e}$	$bs_{B,h}$	$\omega_{2,h}$	interpreting e of B	LP8	Believing that B is feeling *happy* (h)
$srs_{B,h}$		$\omega_{1,h,h}$	interpreting h of B		- from showing emotional by B
srs_{h}		$\omega_{4,h}$	interpreting own h		- from emotion h showed by B
$bs_{B,s}$		$\omega_{2,s,h}$	suppressing belief of s		- from own emotional feeling h
					- decreases by belief state for emotion s
$cs_{selfother,B,e}$	$ps_{comm,B,h}$	$\omega_{6,h}$	controlling communication believing h of B	LP9	Preparing for body state h: communicating that B feels happy: - controlled by self-other distinction
$bs_{B,h}$		$\omega_{5,h}$	suppressing preparation state s of B		- from believing B has emotion h
$ps_{comm,B,s}$		$\omega_{7,s,h}$			- suppressed by preparation state that B has emotion s
$cs_{selfother,B,e}$	$es_{comm,B,h}$	$\omega_{9,h}$	controlling communication executing response	LP10	Expressing communication of body state h of B (communicating that B feels happy) - controlled by self-other distinction
$ps_{comm,B,h}$		$\omega_{8,h}$			- from preparation state for h
$ws_{B,s}$	$ss_{B,s}$	$\omega_{17,s}$	sensing s of B	LP11	Sensing body state s (sad) of person B
$ss_{B,s}$	$srs_{B,s}$	$\omega_{19,s}$	representing s of B	LP12	Representing the stimulus of B showing sad
$srs_{B,e}$	$bs_{B,s}$	$\omega_{2,s}$	interpreting e of B	LP13	Believing that B is feeling *sad* (s)
$srs_{B,n}$		$\omega_{1,s,s}$	interpreting s of B		- from showing emotional by B
$srs_{B,s}$		$\omega_{4,s}$	interpreting own s		- from emotion s showed by B
srs_{s}		$\omega_{2,h,s}$	suppressing belief of h		- from own emotional feeling s
$bs_{B,h}$					- decreases by belief state for emotion h
$cs_{selfother,B,e}$	$ps_{comm,B,s}$	$\omega_{6,s}$	controlling communication believing s of B	LP14	Preparing for body state s: communicating that B feels sad - controlled by self-other distinction
$bs_{B,s}$		$\omega_{5,s,h}$	suppressing preparation state h of B		- from believing B has emotion s
$ps_{comm,B,h}$		$\omega_{7,h,s}$			- suppressed by preparation state that B has emotion h
$cs_{selfother,B,e}$	$es_{comm,B,s}$	$\omega_{9,s}$	controlling communication executing response	LP15	Expressing communication of body state s of B (communicating that B feels sad) - controlled by self-other distinction
$ps_{comm,B,s}$		$\omega_{8,s}$			- from preparation state for s
ws_{h}	ss_{h}	$\omega_{18,h}$	sensing own h	LP16	Sensing body state h (happy) for feeling happy
ss_{h}	srs_{h}	$\omega_{13,h}$	representing h of B	LP17	Representing a *body map* for h: emotion h felt (own feeling of happy)
ps_{h}		$\omega_{14,h}$	predicting h		- from sensing own body state h
					- via as-if body loop for body state h
srs_{h}	ps_{h}	$\omega_{12,h}$	amplifying	LP18	Preparing for body state h: emotional response h (own feeling h) - via emotion integration from own emotion
$srs_{B,h}$		$\omega_{11,h}$	mirroring h of B to own emotional feeling		- via mirroring of emotion that B shows
ps_{h}	es_{h}	$\omega_{15,h}$	Executing emotional response	LP19	Expressing emotional response of h
ws_{s}	ss_{s}	$\omega_{18,s}$	sensing own s	LP20	Sensing body state s (sad), own feeling of sad
ss_{s}	srs_{s}	$\omega_{13,s}$	representing s of B	LP21	Representing a *body map* for s: emotion s felt (own feeling of sad)
ps_{s}		$\omega_{14,s}$	predicting s		- from sensing own body state s
					- via as-if body loop for body state s
srs_{s}	ps_{s}	$\omega_{12,s}$	amplifying	LP22	Preparing for body state s: emotional response s (own feeling s) - via emotion integration from own emotion
$srs_{B,s}$		$\omega_{11,s}$	mirroring s of B to own emotional feeling		- via mirroring of emotion that B shows
ps_{s}	es_{s}	$\omega_{15,s}$	Executing emotional response	LP23	Expressing emotional response of s
es_{h}	ws_{h}	$\omega_{16,h}$	Effectuating h	LP24	Effectuating actual body state
es_{s}	ws_{s}	$\omega_{16,s}$	Effectuating s	LP25	Effectuating actual body state

Table 2
Settings for the scaling factors used and connection weights deviating from 1.

	LP8	LP9	LP13	LP14	LP17	LP18	LP21	LP22
λ	2.2	1.3	1.55	1.3	2	2	2	2

$\omega_{2,h}$	$\omega_{2,s}$	$\omega_{4,h}$	$\omega_{4,s}$	$\omega_{3,s,h}$	$\omega_{3,h,s}$	$\omega_{7,h,s}$	$\omega_{7,s,h}$	$\omega_{6,s}$	$\omega_{6,h}$	$\omega_{9,s}$	$\omega_{9,h}$
0.7	0.05	0.5	0.5	−0.05	−0.05	−0.2	−0.2	0.3	0.3	0.25	0.25

labeled as a sad emotion shown by some person B, and the second simulation has an input labeled as a happy emotion shown by some person B. The simulations are chosen to prove that the model works with different kinds of inputs.

Fig. 2 shows the first simulation of Scenario 1. It can be seen that the states for a person showing emotional ($ws_{B,e}$) and for a person showing a sad face ($ws_{B,s}$) are highly activated at the start (orange lines). Naturally, the sensor states and sensory representation states are

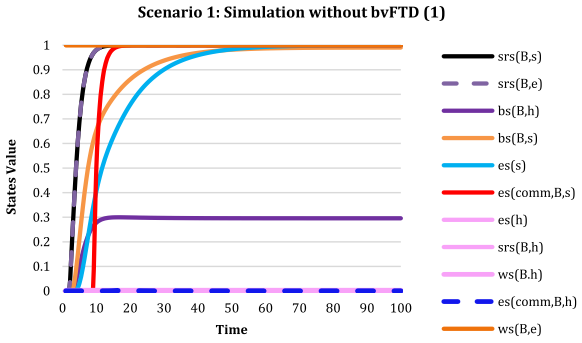

Fig. 2. Simulation results for Scenario 1(1): normal functioning.

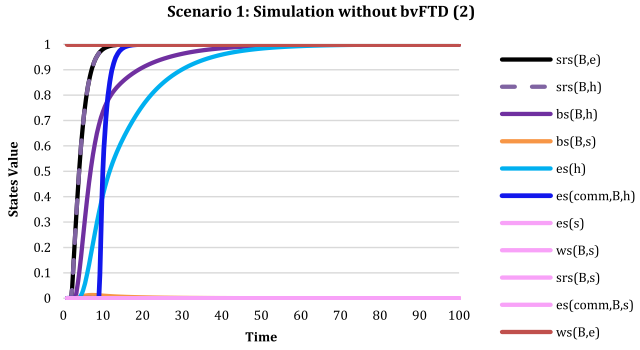

Fig. 3. Simulation results for Scenario 1(2): normal functioning.

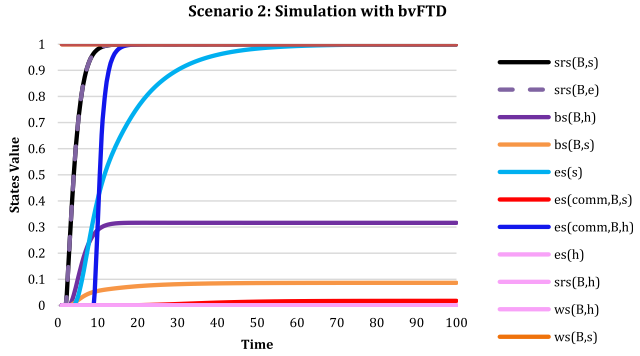

Fig. 4. Simulation results for Scenario 2: the case with bvFTD.

becoming active as well ($srs_{B,e}$ and $srs_{B,s}$) which can be seen by the yellow and black striped lines. The state for the representation of a happy face ($srs_{B,h}$) stays low, visible by the pink striped line. Furthermore, it can be seen that the belief state for recognizing a happy face ($bs_{B,h}$) shows some activation (purple line). This is caused by the fact that the state for recognizing an emotional face is high, but when it becomes clear to the person that the emotion is about a sad emotion, the feeling that it might be a happy emotion is quickly reduced and it can be seen that the communication state for a happy emotion ($es_{comm,B,s}$) stays low (dark blue line). In the end, the person communicates that a sad face has been observed ($es_{comm,B,s}$, red line). Also, the mirror neuron system for the own sad feeling becomes active, showing that emotion contagion takes place for the observed sadness. This can be seen by the activation of es_s which is in the emotion contagion cycle (light blue line). When performing the simulation with the activation of a happy face instead of a sad face at the start, similar results are expected (with the activation of communication a happy face instead of a sad face) as this is how people would normally react. This will be explored in the second simulation.

Fig. 3 shows the second simulation of Scenario 1. It can be seen that the states for a person showing emotional ($ws_{B,e}$) and for a person showing a happy face ($ws_{B,h}$) are highly activated at the start (orange lines) while the state for a person showing a sad ($ws_{B,s}$) face stays inactive (pink line). The process nearly follows the same development over time as the simulation shown in Fig. 2. It can be seen that as a response to the input, the sensory response states become high as well ($srs_{B,e}$ and $srs_{B,h}$). As a response, the belief state that person *B* shows a happy emotion ($bs_{B,h}$) gets highly activated as well. In the end, the communication state for communicating that a happy emotion of person *B* has been experienced ($es_{comm,B,h}$). This simulation also confirms correct behaviour of the model, as it is expected that with an input of emotional and happy, the output of communicating that a happy emotion has been experienced will be activated for normal persons. Therefore, this model shows what is expected of how someone without any impairment, affected by these processes, would interpret an emotion.

For the second scenario, the settings of four weights have been changed. The weights for $\omega_{1,h,h}$, $\omega_{1,s,s}$, $\omega_{4,h}$, and $\omega_{4,s}$ have been set to a connection weight of 0.05. These settings are chosen because the second scenario illustrates the case of a person with bvFTD, which means that those links are damaged and therefore have a low connection strength. Fig. 4 displays the result of the second scenario. In the graph, it can be seen that the external states for showing an emotional face ($ws_{B,e}$) and showing a sad face ($ws_{B,s}$) are high from the start, and are kept high, to simulate their presence (orange lines). However, due to the damaged links, the communication state for saying that a person shows a sad face ($es_{comm,B,s}$, red line) is not activated in the end. However, emotion contagion still causes the own sad feeling (es_s) to develop (activation of light blue line). This can be seen by the red line at the bottom of the graph that stays low throughout the entire simulation, this implies that there is no communication of an observed sad feeling while the light blue line indicates the own sad feeling to be active. In contrast, the communication state for saying that a person shows a happy face ($es_{comm,B,h,}$ dark blue) does get activated while the person never received an input of someone showing a happy face ($ws_{B,h}$), and no contagion of happiness took place (es_h). This can be explained by the fact that the person does recognize that there is an emotion visible (activation of $srs_{B,e}$, yellow line). However, the interpretation of the specific kind of emotion is disrupted. Therefore, the simulation shows the specific case that has been observed in patients: how damaged links can cause someone with bvFTD to misinterpret emotions (Box 1).

An adaptive network model incorporating a therapy

This section describes the adaptive temporal-causal network model for therapy on people with bvFTD. The model is an extension to the computational model proposed in the first part of the report which describes how interpretation of emotions takes place, with a focus on recognizing emotions showed by others. This model also showed how the recognition of emotions can be disturbed in people with bvFTD. Damaged links can cause a patient to incorrectly classify emotions. The extension to the model proposed in this section focuses on the possibility that people with bvFTD receive the rTMS therapy that recovers the damaged links in the network. This could potentially lead to the effect that the links are getting strong enough again to correctly classify emotions.

Fig. 5 gives an overview of the conceptual representation of the model. The links that are marked in red play an important role in the interpretation of emotions by a person, and are damaged (weakened) in persons with bvFTD. When these links are not damaged the model behaves as someone without bvFTD. When these links are damaged the model displays behaviour that has been seen by people with bvFTD as was shown in Part 1.

To introduce the longer term effect of the therapy a Hebbian Learning Rule is applied to all damaged links. With this rule, the weights become adaptive and can become stronger by the effect of

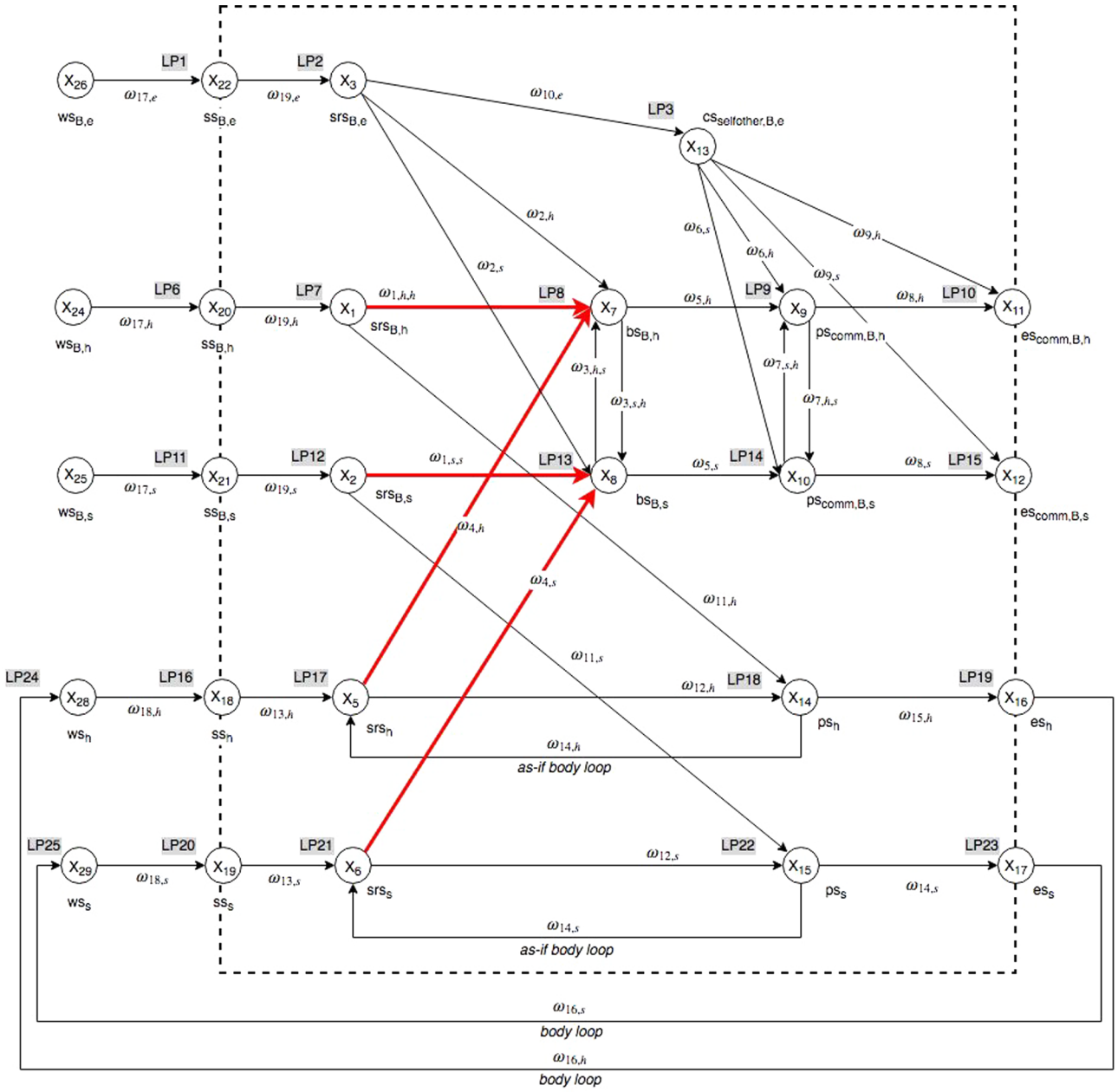

Fig. 5. Overview of the conceptual representation of the model.

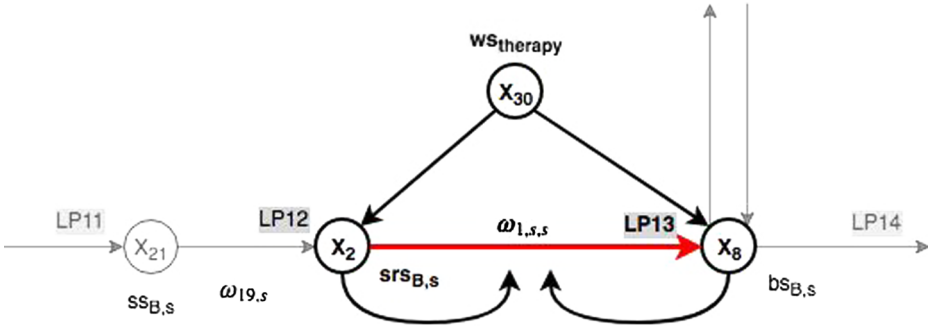

Fig. 6. Hebbian Learning incorporated in the model.

learning. The Hebbian Learning Rule used is numerically described as follows (Treur, 2016b; Gerstner & Kistler, 2002):

$$\omega(t + \Delta t) = \omega(t) + \eta[c_\omega(X_1(t), X_2(t), \omega(t)) - \omega(t)]\Delta t$$

with

$$c_\omega(V_1, V_2, W) = V_1V_2(1 - W) + \mu W$$

where V_1 stands for $X_1(t)$, V_2 for $X_2(t)$, and W for $\omega(t)$. Here η is a learning rate and μ a persistence factor, and X_1, X_2 are the states connected by connection weight ω.

This is incorporated in the model by using the conceptual structure in Fig. 6. The figure shows one of the four places where the Hebbian Learning effect is applied to. An extra state has been added to the model, namely X_{30} which represents the therapy. The therapy can have a state value of either zero or one. Zero when the there is no therapy, one when there is therapy. When the therapy is on it will stimulate the states in the brain area where the damaged parts are. When those get simultaneously activated the connection will become stronger by the Hebbian learning. This will be paired with the input to activate and stimulate the correct connections and areas during the same time. The therapy state X_{30} and its connections is an addition to all the states and connections explained in Table 1.

This Hebbian learning principle is applied to all the areas in the brain where the damaged "red" connections are, visible in Fig. 5. Therefore, the model consists of four of these Hebbian learning connections. By introducing a learning effect for these four connections, the network model becomes an adaptive network model.

The choice for persistence factor μ and learning rate η for the Hebbian learning principle can have big consequences for the simulations of the model and therefore must be chosen carefully and ideally in relation to empirical observations. As such empirical information is not available yet, here it is analysed how variation of these parameter values affects the outcomes of the therapy. The effects of different values for these parameters can be seen in the three examples below. For all simulations, ω_1 is a weight of which the connection is learned by the principle. Weight ω_4 is a connection to which the Hebbian learning principle is applied, but no input is given for connections to which the learning principle never takes place. The first example shows a simulation of one (very long) therapy session with persistence $\mu = 1$ and learning rate $\eta = 0.01$. The result can be seen in Fig. 7. For connection ω_1, the learning effect takes place and reaches a value of about 1 in the end. For the other weight, ω_4, nothing happens and the value stays the same throughout the simulation.

Next, simulation example 2 in Fig. 8 shows a simulation with persistence $\mu = 0.95$ and learning rate $\eta = 0.01$. The only difference to simulation 1 is the persistence factor which has decreased in this simulation. As can be seen, this results in ω_1 increasing slightly less than the simulation in example 1. Next to that, ω_4 shows slight decrease in value as can be explained by the persistence factor being 0.95 resulting in a decay of the connection weight when there is no input to increase by the Hebbian learning effect.

Finally, simulation example 3 shows in Fig. 9 shows a simulation with persistence $\mu = 0.95$ and learning rate $\eta = 0.005$. This example shows the influence of the learning rate η since this is the only difference compared to simulation example 2. As can be seen, in the end the value for ω_1 turns out to be about the same as for ω_1 in example 2. However, due to the lower learning rate, the increase of ω_1 is slower than seen in example 1 and 2.

These examples show how different persistence factors and learning rates can affect the model. Therefore, it shows how these parameters values affect the therapy and how they can and should be chosen in such a manner that the therapy outcomes correspond to what is expected from empirical literature.

Simulation experiments for the adaptive model with therapy

To explore the effects of the incorporated therapy by the adaptive temporal-causal network model described above, again, simulations were performed in Matlab. The simulations show different states of social functioning. First, it shows how damaged connections in the brain as a result of bvFTD cause a dissociation between emotion contagion and facial emotion recognition. Specifically, this is shown by a case in which a patient with bvFTD is confronted by an input that can be labeled as an emotionally sad face. When the patient is asked to communicate the emotion that is experienced, the patient communicates that these must be tears of joy. The incorrect labeling of emotions is an effect of bvFTD. Second, the therapy will be applied to the patient in two different scenarios. The therapy consists of a few sessions to the patient to enhance the damaged links and it is expected that by this therapy the damaged links will become stronger. By the strengthening of these links the patient could be able to correctly classify emotions shown by other persons again.

In this model, the strengths of $\omega_{1,s,s}$, $\omega_{1,h,h}$, $\omega_{4,s}$, and $\omega_{4,h}$ are adapted using the Hebbian Learning rule. The settings for the Hebbian learning rule are different for both scenarios to consider different cases. As before, the simulations have been performed with speed factor $\eta = 0.5$ for all states, $\Delta t = 1$, and the scaling factors as displayed in the upper part of Table 2. One change has been made to the model considering the values displayed in Table 2. In this model, the scaling factor of LP13 has been increased to a value of 2.05. This change has been made because connection $\omega_{4,s}$ can become 1 due to the Hebbian learning effect, while this was 0.5 in the model proposed in Part 1. Therefore, an increase of the scaling factor is necessary. Again, LP10 and LP15 make use of a logistic function with steepness 200 and threshold 0.5. The therapy is applied in sessions of 50 time units alternated by 500 time units rest period in which no inputs are given and no therapy is applied. This process is repeated a number of times until

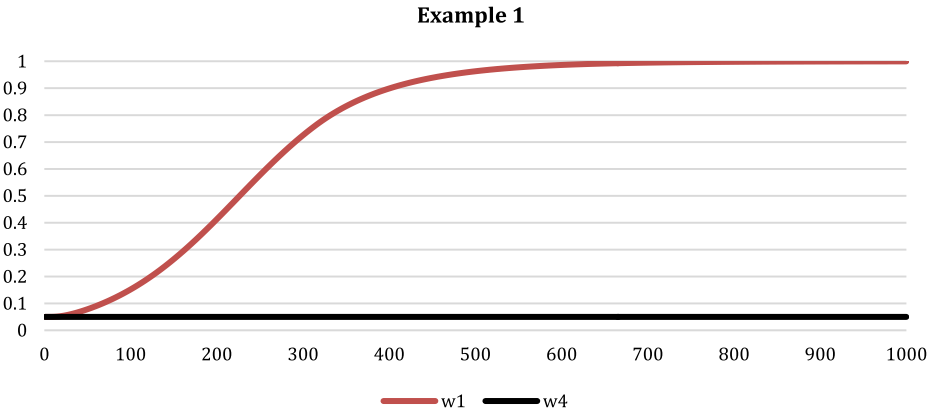

Fig. 7. Example simulation 1 with persistence $\mu = 1$ and learning rate $\eta = 0.01$.

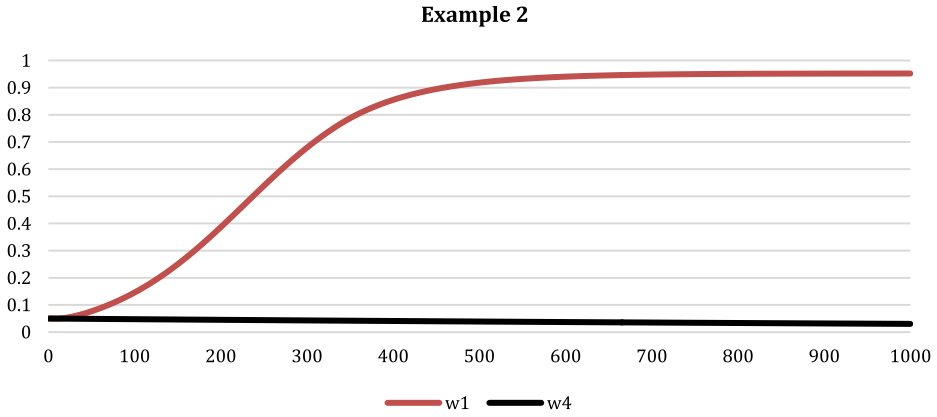

Fig. 8. Example simulation 2 with persistence μ = 0.95 and learning rate η = 0.01.

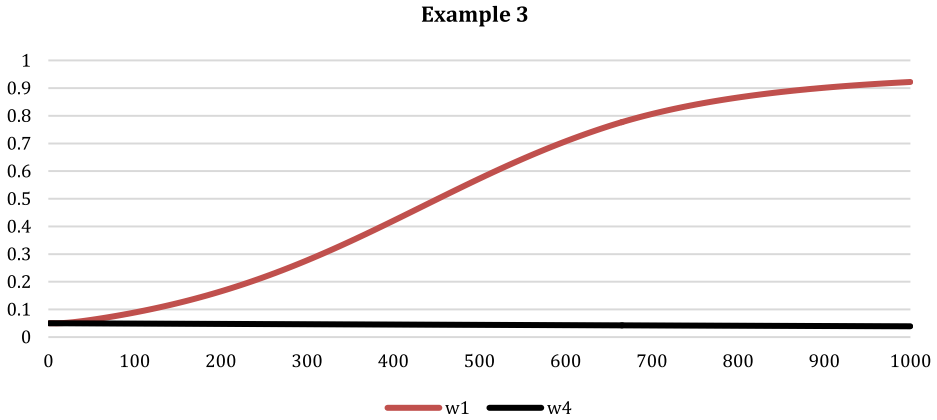

Fig. 9. Example simulation 3 with persistence μ = 0.95 and learning rate η = 0.005.

considered effective.

The graph in Fig. 10 displays the result of a simulation that has been performed before any therapy has been applied. The figure is identical to Fig. 4. However, the graph is reproduced with a different script that has the Hebbian Learning Principle implemented. Therefore, the results are evaluated once again. In Fig. 10, it can be seen that the states $ws_{B,e}$ for a person showing emotional and $ws_{B,s}$ for a person showing a sad face are highly activated at the start and during the whole simulation (dark green lines). This simulates a person *B* showing emotionally sad behaviour. After this, the sensory representation states $srs_{B,e}$ and $srs_{B,s}$ for both observing an emotional face and a sad face become active as well (black and yellow striped lines). The state $srs_{B,h}$ for observing a happy face stays inactive (red line). Although there is no input for a happy face, the sensory representation state for happy and the belief state for a happy face do not become highly active, the communication state $es_{comm,B,h}$ for saying that a happy face is experienced becomes highly active (blue line) and the one $es_{comm,B,s}$ for a sad face does not (red line). This simulation shows how damaged links can cause someone with bvFTD to misinterpret emotions and shows the same behaviour as the simulation represented in Fig. 4. Therefore, the result of this simulation confirms that the adapted script also works as it should.

The next step is to perform simulations where the therapy is applied to the patient. In this first scenario the settings for the Hebbian learning rule are for all weights the same: a maximal connection strength of 1, a learning rate η of 0.01 and a persistence factor μ of 1. Fig. 11 shows the whole process. The graph shows how there are three sessions of therapy (grey line) over a period of 1600 time units. It can be seen that during each session the weights of damaged links with weights $\omega_{1,h,h}$ and $\omega_{4,s}$ become stronger (orange and blue line). Damaged links with weights $\omega_{1,s,s}$ and $\omega_{4,h}$ are not included since they will not become active during any of the simulation scenarios addressed here. However, the same

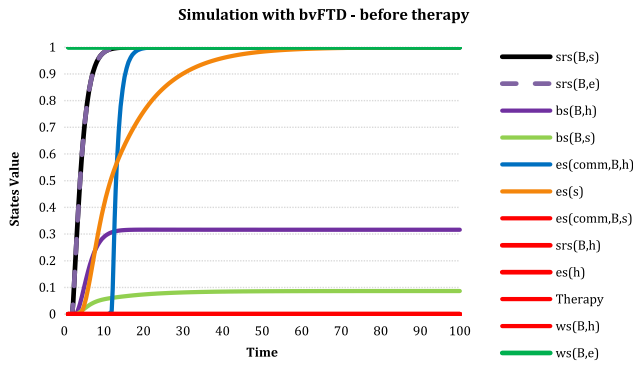

Fig. 10. Simulation results for persons with bvFTD when no therapy is applied.

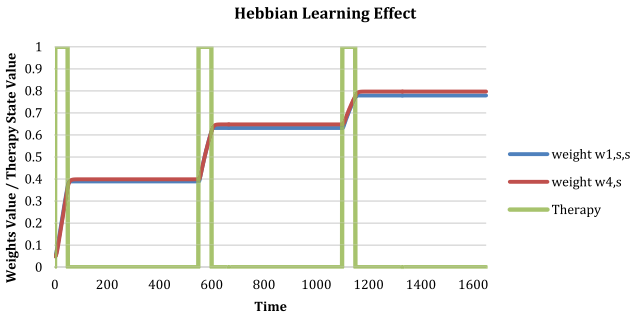

Fig. 11. Simulation results of the applied therapy (1).

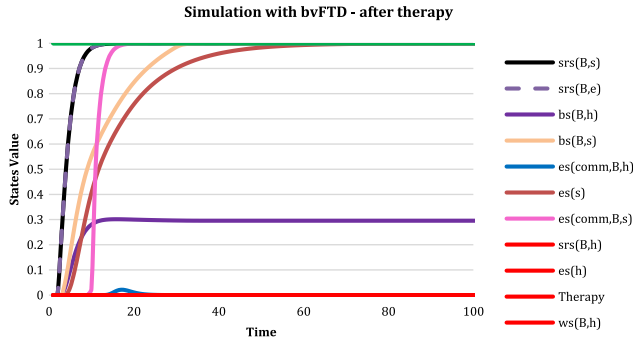

Fig. 12. Simulation results for persons with bvFTD after therapy is applied.

effect can be reached with these weights as well. After three sessions the weights $\omega_{1,h,h}$ and $\omega_{4,s}$ both reach a value of about 0.8. More sessions to obtain a higher value are possible, but after testing, it is found that these values already show the effect that is expected.

These effects can be seen in the graph in Fig. 12. The same input is given as the first simulation that has been performed in Fig. 10. Thus, the states $ws_{B,e}$ for a person showing emotional and $ws_{B,s}$ for a person showing a sad face are highly activated at the start and during the whole simulation (dark green lines). When comparing this graph to the graph in Fig. 10 the effects can be seen clearly. The most important difference is that now, after therapy, the communication state $es_{comm,B,s}$ for saying that a person has been showing a sad emotion becomes active instead of the communication state $es_{comm,B,h}$ for saying that a person has been showing a happy face as was the case before. This is the effect that is expected of how persons normally would react to these stimuli. Therefore, the simulations show how damaged links can be recovered by therapy. However, this case shows how the therapy could work in theory but might not be realistic. The effect of the therapy might not be persistent, and the learning rate might not be as high as is displayed here. Scenario 2 shows another simulation of how the therapy might work, considering a decay and a lower learning rate.

In the second scenario, the settings for the Hebbian learning rule are for all weights the same: a maximal connection strength of 1, a learning rate η of 0.003 and a persistence factor μ of 0.95. These values have been chosen after testing the model multiple times with different configurations and by discussing this with the medical experts who have experience with the patients and the techniques used with this therapy. The graph in Fig. 13 shows the whole process. The graph shows how there are sixteen sessions of therapy over a period of about 8400 time units. When the therapy sessions are applied can be seen by the orange line. It can be seen that during each session the weights of damaged links with weights $\omega_{1,h,h}$ and $\omega_{4,s}$ become stronger (black and blue lines). As the black line shows almost the same development over time as the blue line, it might be not always clearly visible. Each therapy session causes the weights to strongly increase in value. After that, there are 500 time units of no therapy which causes the weights to slowly decrease again due to the fact that the persistence of the learned connections is not equal to 1. As can be seen, over time the effect of the therapy is decreasing in performance. In the end, the gain of the therapy is almost equal to the loss in the period that follows of no therapy. This suggests that after a certain amount of therapy sessions the therapy might become less efficient. If the effect of the therapy is not sufficient yet at that point in time, this will require the sessions to be adapted. This could possibly be accomplished by making the therapy sessions longer, to increase their effect, make the periods between therapy sessions smaller, and if possible to make the decay smaller, or make the sessions stronger, to create a higher learning rate in one session. Damaged links with weights $\omega_{1,s,s}$ and $\omega_{4,h}$ are not included since they will not become active during any of the simulation scenarios addressed here. However, the same effect can be reached with these connections as well. After sixteen sessions of therapy the weights $\omega_{1,h,h}$ and $\omega_{4,s}$ both reach a value of about 0.65.

These effects can be seen in the graph in Fig. 14. The same input is given as the first simulation that has been performed in Fig. 7. Thus, the states $ws_{B,e}$ for a person showing emotional and $ws_{B,s}$ for a person showing a sad face are highly activated at the start and during the whole simulation (dark green lines). When comparing this graph to the graph in Fig. 10 the effects can be seen clearly. The most important difference is that now, after therapy, the communication state $es_{comm,B,s}$ for saying that a person has been showing a sad emotion (pink line) becomes active instead of the communication state $es_{comm,B,h}$ for saying that a person has been showing a happy face (blue line) as was the case before. However, it can be noted that both communication states become highly active. This can be explained by the fact that the connections have reached a weight of about 0.65, which in an ideal situation can be restored to 1 again. As a result, the person has some doubts about which emotion is shown in the beginning, causing both communication states ($es_{comm,B,s}$ and $es_{comm,B,h}$) to be high. However, in the end the person decides this must be a sad emotion expressed by person *B* and this communication state stays high until the end of the simulation ($es_{comm,B,s}$). This is the effect that is expected of how persons normally would react to these stimuli. Therefore, the simulations show how damaged links can be recovered by therapy.

As an addition, a simulation has been performed where the connection weights of the damaged links reach a value of 0.85. This effect could not be reached with the settings of the simulation performed in Figs. 13 and 14. Therefore, the adaptations to the therapy in terms of therapy strength or interval discussed earlier should be explored. This simulation is performed to show the effects when a higher connection

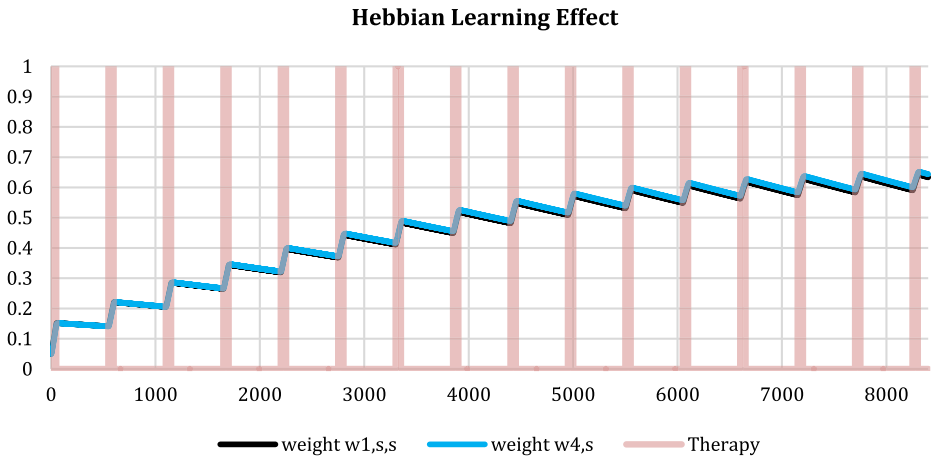

Fig. 13. Simulation results of the applied therapy (2).

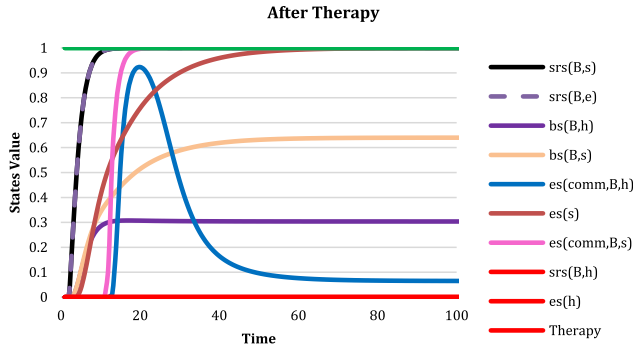

Fig. 14. Simulation results for persons with bvFTD after therapy is applied (1).

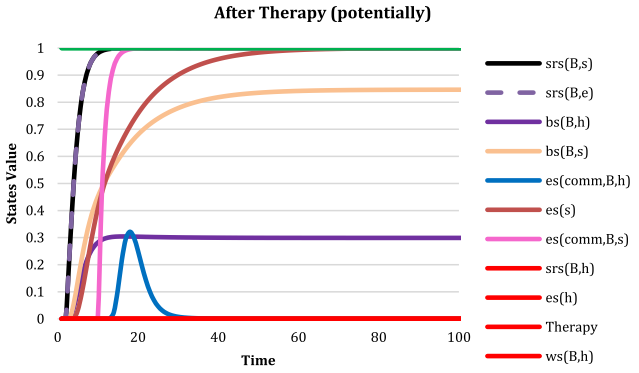

Fig. 15. Simulation results for persons with bvFTD after therapy is applied (2).

strength can be obtained with the therapy. The result can be seen in the graph displayed in Fig. 15. The graph shows that when a higher connection strength is obtained by the therapy, the belief state that person B shows a sad emotion $bs_{B,s}$ becomes higher than shown in Fig. 14, resulting in a stronger connection of recognizing sad emotions and therefore also a better distinction of recognizing happy and sad emotions. Therefore, a lower activation of the communication state for saying that it is a happy emotion $es_{comm,B,h}$ is seen in comparison to the results shown in Fig. 14. This concludes that a connection strength of 0.65 can cause the patient to correctly identify emotions shown by others again (as shown in Fig. 14). However, it is more beneficial if a higher connection strength can be obtained as this will significantly improve the patients' abilities (as has been shown in Fig. 15).

Verification of the network model by mathematical analysis*

Dedicated methods have been developed for temporal-causal network models to verify whether an implemented model shows behaviour as expected; see (Treur, 2016a; Treur, 2016b, Ch 12). In this section equilibria of the designed model are addressed. By Mathematical Analysis their values are found and by comparing them to simulated values the model is verified. Stationary points and equilibria are defined as follows.

A state Y in a temporal-causal network model has a *stationary point* at t if $\mathbf{d}Y(t)/\mathbf{d}t = 0$. A temporal-causal network model is in an *equilibrium state* at t if all states have a stationary point at t. In that case the above equations $\mathbf{d}Y(t)/\mathbf{d}t = 0$ for all states Y are called the *equilibrium equations*. These are general notions, for temporal network models the following simple criterion was obtained in terms of the basic elements defining the network, in particular, the states Y, connection weights $\boldsymbol{\omega}_{X,Y}$ and the combination functions $\mathbf{c}_Y(..)$; see (Treur, 2016a; 2016b, Ch 12).

Criterion for stationary points and equilibria in a temporal-causal network model

A state Y in an adaptive temporal-causal network model with nonzero speed factor has a stationary point at t if and only if

$$\mathbf{c}_Y(\boldsymbol{\omega}_{X_1,Y}X_1(t),\cdots,\boldsymbol{\omega}_{X_k,Y}X_k(t)) = Y(t)$$

where X_1, …, X_k are the states with outgoing connections to Y.

A temporal-causal network model is in an equilibrium state at t if and only if for all states with nonzero speed factor the above criterion holds at t.

Equilibrium equations for an identity function **id(.)** or scaled sum combination function $\mathbf{ssum}_\lambda(..)$ are

$$\mathbf{id}(\omega_{X,Y}X(t)) = \omega_{X,Y}X(t) = Y(t)$$

$$\mathbf{c}_Y(\omega_{X_1,Y}X_1(t),\cdots,\omega_{X_k,Y}X_k(t)) = \frac{(\omega_{X_1,Y}X_1(t)+\cdots+\omega_{X_k,Y}X_k(t))}{\lambda_Y} = Y(t)$$

So, they are linear equations in the state values involved with connection weights and scaling factors as coefficients:

$$\omega_{X,Y}X(t) = Y(t)$$

$$\omega_{X_1,Y}X_1(t) + \cdots+\omega_{X_k,Y}X_k(t) = \lambda_Y Y(t)$$

In the presented model the scaling factors have been set as the sum of the positive weights of the incoming connections; therefore all coefficients are built from connection weights. Using this, the following equilibrium equations for the states were obtained for the presented network model here; to simplify the notation the reference to t has been left out; note that this concerns equilibrium state values here, not state names. Here the connection weights are named as shown in Table 1, and A_1 to A_3 are constants.

$$\mathrm{srs}_{B,h} = A_1 \qquad \mathrm{srs}_{B,s} = A_2 \qquad \mathrm{srs}_{B,e} = A_3$$

$$(\omega_{1,X,X} + \omega_{1,Y,X} + \omega_{2,X} + \omega_{4,X})\mathrm{bs}_{B,X} = \omega_{1,X,X}\mathrm{srs}_{B,X} + \omega_{1,Y,X}\mathrm{srs}_{B,Y} + \omega_{2,X}\mathrm{srs}_{B,e} + \omega_{4,X}\mathrm{srs}_X + \omega_{3,Y,X}\mathrm{bs}_{B,Y}$$

$$(\omega_{5,X} + \omega_{6,X})\mathrm{ps}_{comm,B,X} = \omega_{5,X}\mathrm{bs}_{B,X} + \omega_{6,X}\mathrm{cs}_{selfother,B,e} + \omega_{7,Y,X}\mathrm{ps}_{comm,B,Y}$$

$$(\omega_{8,X} + \omega_{9,X})\mathrm{es}_{comm,B,X} = \omega_{8,X}\mathrm{ps}_{comm,B,X} + \omega_{9,X}\mathrm{cs}_{selfother,B,e}$$

$$\mathrm{cs}_{selfother,B,e} = \omega_{10,e}\mathrm{srs}_{B,e}$$

$$(\omega_{11,X} + \omega_{12,X})\mathrm{ps}_X = \omega_{11,X}\mathrm{srs}_{B,X} + \omega_{12,X}\mathrm{srs}_X$$

$$(\omega_{13,X} + \omega_{14,X})\mathrm{srs}_X = \omega_{13,X}\mathrm{ss}_X + \omega_{14,X}\mathrm{ps}_X$$

$$\mathrm{es}_X = \omega_{15,X}\mathrm{ps}_X$$

$$\mathrm{ss}_X = \omega_{16,X}\mathrm{es}_X$$

Note that in the above equations in the equilibrium state values, variable names X and Y are used that have multiple instances for h (happy) and s (sad). If these equilibrium state values are instantiated and renamed as shown in Table 3, 19 linear equations in X_1 to X_{19} are obtained with coefficients based on the connection weights and the constants A_1 to A_3.

These 19 linear equations can be solved symbolically, for example using the WIMS Linear Solver (see [WIMS, 2018]), thereby obtaining complex algebraic expressions for the equilibrium values, linear in the constants A_1 to A_3 with as coefficients rational (broken) functions in terms of the connection weights. For verification all connection weights have been set as the simulation shown and Table 2. For these connection weight values, the following solution was found in terms of A_1 to A_3:

$$X_1 = \boldsymbol{A_1}$$

* Most parts of this section were adopted from (Commu, Treur, Dols, & Pijnenburg, 2018)

Table 3
State names used in the equilibrium equations.

X_1 $srs_{B,h}$	X_2 $srs_{B,s}$	X_3 $srs_{B,e}$	X_4 srs_h	X_5 srs_s	X_6 $bs_{B,h}$	X_7 $bs_{B,s}$	X_8 $ps_{comm,B,h}$	X_9 $ps_{comm,B,s}$
X_{10} $es_{comm,B,h}$	X_{11} $es_{comm,B,s}$	X_{12} $cs_{selfother,B,e}$	X_{13} ps_h	X_{14} ps_s	X_{15} es_h	X_{16} es_s	X_{17} ss_h	X_{18} ss_s

$$X_2 = \boldsymbol{A}_2$$

$$X_3 = \boldsymbol{A}_3$$

$$X_4 = \boldsymbol{A}_1$$

$$X_5 = \boldsymbol{A}_2$$

$$X_6 = 0.3176815847395451\boldsymbol{A}_3 - 0.02201027146001467\boldsymbol{A}_2 + 0.682318415260455\boldsymbol{A}_1$$

$$X_7 = 0.02201027146001311\boldsymbol{A}_3 + 0.9684519442406457\boldsymbol{A}_2 - 0.02201027146001467\boldsymbol{A}_1$$

$$X_8 = 0.4476266702238825\boldsymbol{A}_3 - 0.1347295404522111\boldsymbol{A}_2 + 0.5402521176549057\boldsymbol{A}_1$$

$$X_9 = 0.1788345672424897\boldsymbol{A}_3 + 0.7656906556392985\boldsymbol{A}_2 - 0.1000466884546121\boldsymbol{A}_1$$

$$X_{10} = 0.5581013361791106\boldsymbol{A}_3 - 0.1077836323617688\boldsymbol{A}_2 + 0.4322016941239245\boldsymbol{A}_1$$

$$X_{11} = 0.3430676537939918\boldsymbol{A}_3 + 0.6125525245114387\boldsymbol{A}_2 - 0.08003735076368973\boldsymbol{A}_1$$

$$X_{12} = \boldsymbol{A}_3$$

$$X_{13} = \boldsymbol{A}_1$$

$$X_{14} = \boldsymbol{A}_2$$

$$X_{15} = \boldsymbol{A}_1$$

$$X_{16} = \boldsymbol{A}_2$$

$$X_{17} = \boldsymbol{A}_1$$

$$X_{18} = \boldsymbol{A}_2$$

For the above connection weight values and values $A_1 = 1$, $A_2 = 0$, and $A_3 = 1$, the solution was found shown in the third and sixth row of Table 4.

A logistic function with steepness 200 and threshold 0.625 applied to the communication execution states X_{10} and X_{11} (multiplied by the scaling factor 1.25 to undo the scaling) provides $X_{10} = 1$, and $X_{11} = 2.613\ 10^{-21}$. Similarly, for other values of A_1 to A_3, the equilibrium values have been found.

For example, for $A_1 = 0$, $A_2 = 0$, $A_3 = 1$, it was found

$X_6 = 0.3176815847395451$

$X_7 = 0.02201027146001467$

$X_8 = 0.4476266702238826$

$X_9 = 0.1788345672424908$

$X_{10} = 0.5581013361791062$

$X_{11} = 0.3430676537939928$

Here a logistic function with steepness 200 and threshold 0.625 was applied to the communication execution states X_{10} and X_{11} multiplied by the scaling factor 1.25 to undo the scaling which provides $X_{10} = 1$, and $X_{11} = 0$.

For $A_1 = 0$, $A_2 = 1$, $A_3 = 1$, it was found

$X_6 = 0.2956713132795305$

$X_7 = 0.9904622157006603$

$X_8 = 0.3128971297716712$

$X_9 = 0.9445252228817893$

$X_{10} = 0.4503177038173369$

$X_{11} = 0.9556201783054313$

Again here a logistic function with steepness 200 and threshold 0.625 was applied to the communication execution states X_{10} and X_{11} multiplied by the scaling factor 1.25 to undo the scaling which provides $X_{10} = 1$, and $X_{11} = 0$. All these values have been checked with the values of the simulation scenarios and were found very accurate (deviations less than 0.001). This provides evidence that the implemented model does what is expected.

Also the equilibria for the adaptive model have been analysed. Application of the stationary point criterion on the Hebbian learning parts of the model is as follows. Recall that for that case the combination function is

$$\mathbf{hebb}_\mu(V_1, V_2, W) = V_1V_2(1 - W) + \mu W$$

where V_1 refers to $X_1(t)$, V_2 refers to $X_2(t)$, and W refers to $\omega_{X_1,X_2}(t)$. Based on this, according to the stationary point criterion in an equilibrium it holds

$$X_1(t)X_2(t)\big(1 - \omega_{X_1,X_2}(t)\big) + \mu\omega_{X_1,X_2}(t) = \omega_{X_1,X_2}(t)$$

$$X_1(t)X_2(t)\big(1 - \omega_{X_1,X_2}(t)\big) = (1 - \mu)\omega_{X_1,X_2}(t)$$

$$X_1(t)X_2(t) - X_1(t)X_2(t)\omega_{X_1,X_2}(t)) = (1 - \mu)\omega_{X_1,X_2}(t)$$

$$X_1(t)X_2(t) = [X_1(t)X_2(t) + (1 - \mu)]\omega_{X_1,X_2}(t)$$

This provides the following relation for $\omega_{X_1,X_2}(t)$:

$$\omega_{X_1,X_2}(t) = \frac{X_1(t)X_2(t)}{X_1(t)X_2(t) + (1-\mu)} = \frac{1}{1 + \frac{1-\mu}{X_1(t)X_2(t)}} \qquad (\text{when} X_1(t)X_2(t) > 0)$$

This is monotonically increasing in $X_1(t)X_2(t)$; the maximal value occurs when $X_1(t) = 1$ and $X_2(t) = 1$, and is

$$\omega_{X_1,X_2}(t) = \frac{1}{2-\mu}$$

Therefore, for example, in the simulations with $\mu = 0.95$, it should

Table 4
Results of the mathematical analysis.

X_1 $srs_{B,h}$ 1	X_2 $srs_{B,s}$ 0	X_3 $srs_{B,e}$ 1	X_4 srs_h 1	X_5 srs_s 0	X_6 $bs_{B,h}$ 1	X_7 $bs_{B,s}$ 0	X_8 $ps_{comm,B,h}$ 0.987879	X_9 $ps_{comm,B,s}$ 0.078788
X_{10} $es_{comm,B,h}$ 0.990303	X_{11} $es_{comm,B,s}$ 0.263030	X_{12} $cs_{selfother,B,e}$ 1	X_{13} ps_h 1	X_{14} ps_s 0	X_{15} es_h 1	X_{16} es_s 0	X_{17} ss_h 1	X_{18} ss_s 0

be expected that the values of the adaptive connections will never exceed 1/[2–0.95] = 0.95238. This can indeed be observed in the simulations.

Discussion

In this paper, first a temporal-causal network model was introduced that describes the interpretation of emotions shown by others. The model can also show cases in which the interpretation of emotions is incorrect, as can be the case of persons with bvFTD; this is based on the assumption that it is at least observed that there is an emotional face, although the specific type of emotion is not recognized correctly. Several simulations have been performed to test the model in both these behaviours. In the presented scenario for a person with bvFTD it was shown how an observed sad face led to contagion of sadness by the mirror system in a correct way, but at the same time the emotional face was nevertheless not recognized as sad, but instead as happy. A mathematical analysis was done confirming the simulation outcomes; this gave evidence that the model as implemented does what it is meant to do.

By comparing the results of the model to the case it can be concluded that the model can correctly simulate behaviour shown by the patient with bvFTD as described in the case in Box 1. Next to that, it can also show how people without any damaged connections would respond to the input.

Next, the paper addresses an extension to the temporal-causal model by obtaining an adaptive network model for the effects of a therapy. It addresses a therapy that might improve the damaged connections in the brain that come with bvFTD. The extended model shows how Repetitive Transcranial Magnetic Therapy (rTMS) can improve the network connections and, in the end, cause a patient to (partly) retain the damaged connections. The two different scenarios show how after several therapy sessions, the connections have improved in such a way that the patient will be able to correctly classify experienced emotions by others again. The first scenario showed how the therapy could work best case scenario. However, this scenario might be too optimistic and therefore a second scenario has been performed. The second scenario also showed how the therapy can improve the connections but due to a decay and a lower learning rate this would cost a lot more time. In the end, for all scenarios, differences between before and after the therapy are clear: certain functions work again after therapy.

However, no real data is available yet to support the model. It could be that the rate of the learning effect is not the exact same number as was used in the simulation scenario. This number can be higher, when the learning effect is stronger, or lower, when the learning effect is slower. This also changes the outcomes in terms of how many sessions are needed to get the desired effect, which means that a different number of sessions are needed to get to the same effect. Also, this model assumes a persistence of 1; meaning that when the improvement of the connection is obtained, it will be persistent, while it might be the case that there is a small decay on the effect. When real data is obtained, all such changes can be easily incorporated in the model as the model stands on its own and the parameters are easily adjusted.

Conclusion

Both models have proven to do what they were designed for. The model first introduced shows a temporal-causal network model that describes how emotions shown by others are interpreted. On top of that, it is shown that in persons with bvFTD certain links within this process are damaged, causing the patient to incorrectly interpret emotions; an example case of this is explained in Box 1. A paper on this model is (Commu et al., 2018). The adaptive extension to the model introduced shows how rTMS therapy can be used to restore the damaged connections and causing the patient to interpret emotions correctly again.

Both models can be applied as a basis for human-like virtual agents, for example, to obtain a virtual patient model to study the way in which recognition of emotions can deviate for certain types of persons. In addition they can be applied to study how to potentially enhance the recognition of emotions when damaged, as was shown in particular by the second model. However, more therapies or techniques can be implemented in the model to explore more possibilities. In further research real data can be used to test the model in more detail. Brain activity could be measured to get real data to use as input for the model and get patterns of how states are activated over time. This could help by tuning the parameters of the model to be even more human-like. Furthermore, more scenarios or cases could be simulated to analyse more and different outcomes of the model. In future extensions of the model, more emotions than sad and happy can also be addressed. The presented models focus specifically on the social cognition disturbances in people with bvFTD. Other symptoms mentioned in Section 1 can also be potential subjects to extend the model or even create new models within the subject of bvFTD. As a conclusion, the created models show the process of emotion recognition and a therapy. For future work, the next step is to obtain real data that can be used to finetune the models and eventually insert patient data into the model.

References

Antczak, J., Kowalska, K., Klimkowicz-Mrowiec, A., Wach, B., Kasprzyk, K., Banach, M., Rzeźnicka-Brzegowy, K., Kubica, J. L., & Słowik, A. (2018). Repetitive transcranial magnetic stimulation for the treatment of cognitive impairment in frontotemporal dementia: an open-label pilot study. *Neuropsychiatric Disease and Treatment, 13*(1), 749–755. https://doi.org/10.2147/NDT.S153213 eCollection 2018.

Alzheimer Nederland (2017). Cijfers en feiten over dementie (Factsheet). https://www.alzheimer-nederland.nl/sites/default/files/directupload/factsheet-dementie-algemeen.pdf.

Boxer, A. L., & Boeve, B. F. (2007). Frontotemporal dementia treatment: Current symptomatic therapies and implications of recent genetic, biochemical, and neuroimaging studies. *Alzheimer Disease & Associated Disorders, 21*(4), S79–S87.

Commu, C., Treur, J., Dols, A., & Pijnenburg, Y. (2018). A Computational Network Model for the Effects of Certain Types of Dementia on Social Functioning. In N. T. Nguyen, E. Pimenidis, Z. Khan, & B. Trawinski (Eds.). *Computational Collective Intelligence: Proc. of the 10th International Conference on Computational Collective Intelligence, ICCCI'18, vol. 1. Lecture Notes in Artificial Intelligence* (pp. 119–133). Springer Publishers.

Damasio, A. R. (1994). *Descartes' error: emotion, reason, and the human brain.* New York: Quill Publishing.

Damasio, A. R. (1999). *The feeling of what happens: body and emotion in the making of consciousness.* Harcourt Incorporated.

Damasio, A. R. (2018). *The strange order of things: life, feeling, and the making of cultures.* Knopf Doubleday Publishing Group.

de Waal, F. B. M. (2009). *The age of empathy.* New York: Random House.

Eldaief, M. C., Press, D. Z., & Pascual-Leone, A. (2013). Transcranial magnetic stimulation in neurology a review of established and prospective applications. *Neurology: Clinical Practice.* https://doi.org/10.1212/01.CPJ.0000436213.11132.8e.

Elder, G. J., & Taylor, J. P. (2014). Transcranial magnetic stimulation and transcranial direct current stimulation: Treatments for cognitive and neuropsychiatric symptoms in the neurodegenerative dementias? *Alzheimer's Research & Therapy, 6*(5), 74.

Eslinger, P. J., Moore, P., Antani, S., Anderson, C., & Grossman, M. (2012). Apathy in frontotemporal dementia: Behavioral and neuroimaging correlates. *Behavioural Neurology, 25*(2), 127–136.

Gerstner, W., & Kistler, W. M. (2002). (2002) Mathematical formulations of Hebbian learning. *Biological Cybernetics, 87*, 404–415.

Gossink, F., Schouws, S., Krudop, W., Scheltens, P., Stek, M., Pijnenburg, Y., & Dols, A. (2018). Social cognition differentiates behavioral variant frontotemporal dementia from other neurodegenerative diseases and psychiatric disorders. *The American Journal of Geriatric Psychiatry, 26*(5), 569–579.

Iacoboni, M. (2009). *Mirroring people: The new science of how we connect with others.* Farrar: Straus and Giroux (2009).

Ibanez, A., & Manes, F. (2012). Contextual social cognition and the behavioral variant of fronto-temporal dementia. *Neurology, 78*(17), 1354–1362. https://doi.org/10.1212/WNL.0b013e3182535d0c.

Kumfor, F., & Hodges, J. R. (2017). Social cognition in frontotemporal dementia proceedings: Special lecture neuropsychology association of japan 40th annual meeting. *Japanese Journal Neuropsychology, 33*(1), 9–24 https://doi.org/10.20584/neuropsychology.33.1_9 (2017).

Lanata, S. C., & Miller, B. L. (2016). The behavioural variant frontotemporal dementia (bvFTD) syndrome in psychiatry. *Journal Neurology Neurosurgery Psychiatry, 87*(5), 501–511.

Piguet, O., Hornberger, M., Mioshi, E., & Hodges, J. R. (2011). Behavioural-variant frontotemporal dementia: Diagnosis, clinical staging, and management. *Lancet Neurology, 10*(2), 162–172. https://doi.org/10.1016/S1474-4422(10)70299-4.

Piguet, O., & Hodges, J. R. (2013). Behavioural-variant frontotemporal dementia: An update. *Dementia & Neuropsychologia, 7*(1), 10–18.

Rascovsky, K., Hodges, J. R., Knopman, D., Mendez, M. F., Kramer, J. H., Neuhaus, J., ... Hillis, A. E. (2011). Sensitivity of revised diagnostic criteria for the behavioural variant of frontotemporal dementia. *Brain, 134*(9), 2456–2477.

Slotema, C. W., Dirk Blom, J., Hoek, H. W., & Sommer, I. E. (2010). Should we expand the toolbox of psychiatric treatment methods to include Repetitive Transcranial Magnetic Stimulation (rTMS)? A meta-analysis of the efficacy of rTMS in psychiatric disorders. *Journal of Clinical Psychiatry, 71*(7), 873.

Sturm, V. E., Yokoyama, J. S., Seeley, W. W., Kramer, J. H., Miller, B. L., Katherine, P., & Rankin, K. P. (2013). Heightened emotional contagion in mild cognitive impairment and Alzheimer's disease is associated with temporal lobe degeneration. *PNAS, 110*(24), 9944–9949 www.pnas.org/cgi/doi/10.1073/pnas.1301119110.

Treur, J. (2016a). Verification of temporal-causal network models by mathematical analysis. *Vietnam Journal Computer Science, 3*, 207–221.

Treur, J. (2016b). *Network-oriented modeling: addressing complexity of cognitive, affective and social interactions.* Springer Publishers.

Treur, J. (2018). *The Ins and outs of network-oriented modeling: From biological networks and mental networks to social networks and beyond. Paper for keynote lecture at ICCCI'18. Transactions on computational collective intelligence.* Springer Publishers, in press.

Wassermann, E. M. (1998). Risk and safety of repetitive transcranial magnetic stimulation: Report and suggested guidelines from the International Workshop on the Safety of Repetitive Transcranial Magnetic Stimulation, June 5–7, 1996. *Electroencephalography and Clinical Neurophysiology/Evoked Potentials Section, 108*(1), 1–16.

[WIMS, 2018] Web Interactive Multipurpose Server; Linear Solver: https://wims.unice.fr/wims/wims.cgi?session=K06C12840B.2&+lang=nl&+module=tool%2Flinear%2Flinsolver.enm.